Acta Chemica Scandinavica, 1998: 52: 733–744
Printed in UK – all rights reserved

ACTA
CHEMICA SCANDINAVICA
ISSN 0904–213X

Properties of $LaCo_{1-t}Cr_tO_3$. IV. Structure and Magnetism

B. Gilbu Tilset,[a] H. Fjellvåg,[a] A. Kjekshus[a,*] and B. C. Hauback[b]

[a]Department of Chemistry, University of Oslo, N-0315 Oslo, Norway and [b]Institute for Energy Technology, N-2007 Kjeller, Norway

Tilset, B. G., Fjellvåg, H., Kjekshus, A. and Hauback, B. C., 1998. Properties of $LaCo_{1-t}Cr_tO_3$. IV. Structure and Magnetism. – Acta Chem. Scand. 52: 733–744. © Acta Chemica Scandinavica 1998.

The structural and magnetic properties of the perovskite-type $LaCo_{1-t}Cr_tO_3$ phase ($0 \leqslant t \leqslant 1$) have been studied by powder X-ray and neutron diffraction and by magnetic susceptibility measurements between 5 and ca. 1100 K. In the Co-rich composition range with an $LaAlO_3$-type atomic arrangement ($0 \leqslant t < \sim 0.7$ at $T < 200$ K), $LaCo_{1-t}Cr_tO_3$ undergoes a number of composite 'spin' conversion processes. In the Cr-rich composition range with a $GdFeO_3$-type atomic arrangement ($\sim 0.7 < t \leqslant 1$ at $T < 200$ K), an antiferromagnetic ordering of the 'spins' is adopted. The antiferromagnetic ordering also extends into the $LaAlO_3$-type region and is observed in $LaCo_{0.60}Cr_{0.40}O_3$, with a superimposed ferromagnetic component below ca. 100 K according to magnetic susceptibility measurements. The findings are discussed in relation to current apprehensions of the properties of the end phases $LaCoO_3$ and $LaCrO_3$.

The perovskite-type $LaCoO_3$–$LaCrO_3$ solid-solution system is of considerable interest owing to its intriguing physical properties and the potential use of such materials as heterogeneous catalysts, components for solid oxide fuel cells, etc. The present contribution is part of a project aimed at determining the effect of physical and chemical properties on the catalytic activity for CO oxidation. Throughout the $LaCo_{1-t}Cr_tO_3$ phase, the catalytic, physical and chemical properties vary appreciably.[1–3] In the preceding contributions we have reported on structural properties,[1] thermal expansion,[1] IR characteristics,[1] reduction,[2] reoxidation[2] and catalytic activity.[3] There is no obvious correlation between activity for CO oxidation and bulk properties like crystal structure, electric conductivity or magnetic moment at high temperatures.[3] The present paper focuses on magnetic properties at low and high temperatures and provides data for crystal and magnetic structures.

Lanthanum cobalt oxide, $LaCoO_3$, has repeatedly been studied. Various sorts of experiments have been conducted to elucidate its intricate magnetic and electronic properties, including magnetic susceptibility,[4–17] electric conductivity,[4,6,8–11,14–16,18,19] Seebeck coefficient,[4,10,19] neutron diffraction,[20,21] polarized neutron paramagnetic scattering,[22,23] Mössbauer spectroscopy,[9] X-ray absorption spectroscopy (XAS),[17,24–27] X-ray photoelectron spectroscopy (XPS),[17,27–31] adiabatic heat capacity[32] and various other experimental and calculation techniques.[33–38] The selection of references considered so far is not exhaustive, and a remarkable number of papers have in fact appeared after this manuscript was finalized and even after it was submitted. However, the recent developments do not change the essence of our scientific message. A few additional references are moreover introduced in the discussion. Despite all endeavours, crucial questions regarding the electronic properties of $LaCoO_3$ must still be considered as open.

The situation is much simpler for the other end member of the solid-solution series, $LaCrO_3$, which is a semiconducting antiferromagnet at low temperatures.[39,40] Its crystal structure is orthorhombic ($GdFeO_3$-type, space group *Pnma*), and the magnetic ordering below $T_N = 282$ K is basically of the G_x type.[20,41,42] The orthorhombic regime covers the range $\sim 0.8 < t \leqslant 1.00$ of $LaCo_{1-t}Cr_tO_3$ at ambient.[1] A narrow miscibility gap separates it from the rhombohedral solid-solution regime ($LaAlO_3$-type, space group $R\bar{3}c$[7,21]) extending from $LaCoO_3$.[1,43,44]

The magnetic properties of $LaCoO_3$ are quite intricate and are *inter alia* manifested in the temperature dependence of the magnetic susceptibility. In discussing the magnetic properties of $LaCoO_3$, it is appropriate to consider four temperature regimes, $T < \sim 100$ K, $\sim 100 < T < \sim 400$ K, $\sim 400 < T < \sim 600$ K and $T > \sim 600$ K. The magnetic properties at low temperatures depend on the sample quality, and are affected by, e.g., repeated firings and regrindings.[7,12,14]

* To whom correspondence should be addressed.

In the interval ca. 100–400 K and for temperatures above some 600 K, the magnetic susceptibility obeys the Curie–Weiss relationship.[4,6,10,14] The reported effective paramagnetic moments vary considerably, 3.1 and 4.0 μ_B being representative values for the two regimes. $LaCoO_3$ is considered to undergo a spin transition at around 500 K.[4,6,14,16–18,26,30,31] Early reports on yet another (electronic) transition at 1210 K have later proved to refer to Co_3O_4 impurities in the samples.[14,18,19] It has been suggested from powder X-ray diffraction (PXD) data that a symmetry reduction to $R\bar{3}$ occurs in a temperature interval around 600 K, owing to crystallographic ordering of low- and high-spin cobalt(III) species.[8] However, the support from powder neutron diffraction (PND) data is lacking.[20] On the other hand, Mössbauer[9] and EXAFS[34] data indicate the presence of two different Co species at high temperatures. Recently it has been suggested that the spin ordering is not of a static nature with long-range order, but rather of a dynamic short-range nature.[14] The thermal expansion shows an anomalous increase in the temperature interval 500–700 K.[1,16] Differential scanning calorimetry (DSC),[1] differential thermal analysis (DTA)[8] and recent adiabatic calorimetry data[32] show a substantial excess entropy in an interval around 500 K. In this temperature range, the electrical conductivity is essentially independent of the oxygen partial pressure[17] and increases by about two orders of magnitude between 350 and 750 K.[4,10,11,15–19] On this basis, $LaCoO_3$ has been classified as a material which undergoes a higher-order, temperature-induced semiconductor-to-metal transition. Several qualitative band structure schemes have been forwarded,[14,19,24–26,28,31,33,35] and approximate band structure calculations are at hand.[27,29,30,36,38]

Below ca. 100 K, the reported magnetic susceptibility of $LaCoO_3$ exhibits a broad minimum. However, no magnetic order has been observed down to 4.2 K by PND.[20,21] It is therefore believed that the ground state of $LaCoO_3$ at 4.2 K is non-magnetic ($S=0$; $^1A_{1g}$) with a transition via an intermediate state ($S=1$, $^3T_{1g}$) to a metallic, high-spin state ($S=2$; $^5T_{2g}$) on heating.[32] Several authors maintain that the spin transition to the intermediate state occurs around 100 K. Paramagnetic neutron scattering data appear to support this view.[22,23] Furthermore, a smaller anomaly in the thermal expansion occurs in this temperature range.[23] On the other hand, recent XAS[26] and XPS[27] data indicate no transition below 300 K. Adiabatic calorimetry data[32] show only indistinct evidence of a heat capacity (c_p) peak below ca. 350 K, in marked contrast to the pronounced c_p peak centered around ca. 500 K.

In the present study, the properties of $LaCoO_3$ are followed into the solid-solution range of $LaCo_{1-t}Cr_tO_3$. Magnetic properties are probed by magnetic susceptibility for zero field cooled (ZFC) and field cooled (FC) samples; magnetic and crystal structures are derived from PND data. The different cobalt species are denoted by notations which give formal oxidation (usually Co^{3+}) and spin (LS for low-spin, IS for intermediate-spin and HS for high-spin) state.

Experimental

Samples (12–15 g) of $LaCo_{1-t}Cr_tO_3$, $t=0.00$, 0.10, 0.40, 0.90 and 1.00, for PND studies were prepared by multiple firings of citrate gels, in general following the procedure given in Ref. 1. After decomposition of the organic precursor at 723 K, the samples were fired in air at 1073 K for 30 h, followed by slow cooling (1 K min^{-1}) to room temperature. The samples were ground in a planetary mill and the firing process repeated. In addition, small-scale samples prepared during the work with Ref. 1 were used for magnetic susceptibility measurements. La_2O_3 (99.98%, Fluka), $Co(CH_3COO)_2 \cdot 4H_2O$ (>99.0%, Fluka), CrO_3 (>99%, Merck) and $C_3H_4(OH)(COOH)_3 \cdot H_2O$ (reagent grade, Sturge Biochemicals) were used as reactants. Prior to use, any hydrated and/or carbonated species present in the lanthanum oxide were removed by heating to 1273 K. The actual metal contents of the cobalt acetate and the chromium oxide were determined thermogravimetrically.

All samples were characterized by PXD. The products were phase pure within the detection limits of the potential contaminants (0.3 wt% for La_2O_3 and Co_3O_4),[1] and gave the same unit-cell dimensions as samples prepared previously.[1–3] DTA of $LaCoO_3$ showed no peak that could be referred to decomposition of Co_3O_4.

Magnetic susceptibility was measured between 290 and 980 K with a Faraday balance (maximum field 8 kOe) on increasing and decreasing temperature. The powder samples (35–70 mg) were vacuum sealed in silica-glass ampoules. Between 5 and 325 K, magnetization data were recorded with a SQUID magnetometer (MPMS, Quantum Design; 0.010–50 kOe). The samples (17–67 mg) were contained in gelatin capsules. Diamagnetic corrections were made for the ampoules/capsules and core electron contributions.

PND data were collected with the OPUS III two-axis diffractometer at the JEEP II reactor, Kjeller, at a wavelength of $\lambda=182.5$ pm. Data were collected between $2\Theta=5$ and 95° in steps of $\Delta(2\Theta)=0.05°$. The powder samples were pressed into pellets and loaded into cylindrical Al containers. Experiments were conducted at temperatures between 11 and 293 K, using a Displex cooling system with a Lake Shore DRC 82C temperature controller. Corrections were made for weak $\lambda/2$ and $\lambda/3$ contributions. Regions with reflections from Al of the sample container were excluded from the refinements, except when Al peaks overlapped those from the sample. In the latter cases, the contribution from Al was subtracted from the diffractogram. Additional PND data were collected at 293 K for $LaCoO_3$ and $LaCo_{0.60}Cr_{0.40}O_3$ with the TAS III instrument at the DR3 reactor at Risø National Laboratory, Roskilde, Denmark, at a wavelength of 145.05 pm. The range 10–115.79° was covered by moving the detector bank,

Table 1. Structural parameters for rhombohedral $LaCo_{1-t}Cr_tO_3$ as determined from PND.[a]

t	T/K	a/pm	α/°	x_O
0.00	12	534.68(4)	60.976(2)	0.1973(2)
0.00	293	538.38(5)	60.788(2)	0.1999(2)
0.00	*293*	*537.85(2)*	*60.800(2)*	*0.2001(3)*
0.10	11	535.85(4)	60.941(2)	0.1972(2)
0.10	293	539.00(4)	60.778(2)	0.1993(2)
0.40	11	538.87(4)	60.891(2)	0.1965(2)
0.40	293	540.68(4)	60.771(2)	0.1980(2)
0.40	*293*	*539.15(3)*	*60.773(3)*	*0.1988(4)*
0.40	*673*	*543.87(4)*	*60.601(4)*	*0.1994(5)*
0.40	*1073*	*549.38*	*60.461*	*0.2028(6)*

[a]Space group $R\bar{3}c$; La in 2a, Co/Cr in 2b, and O in 6e. R_n ranges between 0.024 and 0.042 and R_p between 0.053 and 0.072. Numerals in italics refer to data obtained at Risø. Calculated standard deviations in parantheses.

consisting of twenty ^{3}He detectors, 5.2897° during 100 steps. Diffractograms for $LaCo_{0.60}Cr_{0.40}O_3$ were in addition obtained at 673 and 1073 K, using a furnace where the sample was filled in an open silica glass ampoule.

Profile refinements were performed using the Hewat[45] and MPROF[46] versions of the Rietveld program.[47] Scattering lengths $b_{La}=8.27$, $b_{Co}=2.78$, $b_{Cr}=3.53$ and $b_O=5.80$ fm were taken from Ref. 48. Magnetic form factors for Cr^{3+} were taken from Ref. 49. During the refinements for the rhombohedral (orthorhombic) samples, two (three) unit-cell parameters, one (seven) positional parameters, two (three) magnetic moments, three half-width parameters, three isotropic temperature factors, the counter zero-point and the overall scale factor entered as free variables. Interatomic distances at 298 K were calculated from atomic coordinates deduced from PND data and unit-cell dimensions determined by PXD.

Results

Crystal structure data. The PXD and PND data show unambiguously that Co and Cr are randomly distributed over the octahedral site in the crystal structure(s) of $LaCo_{1-t}Cr_tO_3$. For the rhombohedral regime a satisfactory fit was obtained for refinements according to space group $R\bar{3}c$. The possibility of Co/Cr ordering was carefully checked for $t=0.40$ at 298, 673 and 1073 K by refinements in terms of space group $R\bar{3}$, but no indication of symmetry reduction was found; inter alia, (111) was not observed. However, TEM data for $LaCoO_3$ clearly showed the presence of *hhl* reflections with $l=2n+1$, thus violating the extinction rules of space group $R\bar{3}c$.[50] The excellent fit obtained for the PND data according to space group $R\bar{3}c$ suggests very strongly that this feature is caused by, e.g., small fluctuations in electron density, minor amounts of unevenly distributed vacancies or multiple electron scattering. For the orthorhombic regime, refinements were based on the space group *Pnma*. Refined parameters are listed in Tables 1 and 2; interatomic distances in Tables 3 and 4.

The La–O and Co/Cr–O interatomic distances vary smoothly with the composition parameter t. From the distances, the valences of Cr/Co and La can be estimated using the bond-valence concept.[51] There is a certain discrepancy between calculated and expected valences. If interatomic distances with bond valences <0.114 are considered to be non-bonding,[52] the three long La–O distances (>299 pm) will not contribute. The bond-valences

Table 3. Interatomic distances (in pm) for rhombohedral $LaCo_{1-t}Cr_tO_3$.[a]

t	T/K	Co/Cr–O	La–O (6×)	La–O (3×)	La–O (3×)
0.00	12	192.6	268.9	242.7	299.9
0.00	293	193.2	270.3	244.9	299.4
0.00	*293*	*193.2*	*270.3*	*245.0*	*299.3*
0.10	11	192.9	269.5	243.1	300.4
0.10	293	193.3	270.4	244.6	299.8
0.40	11	194.0	271.0	243.8	302.3
0.40	293	194.0	271.3	244.6	301.4
0.40	*293*	*194.0*	*271.3*	*245.1*	*301.0*
0.40	*673*	*195.4*	*273.6*	*247.0*	*302.7*
0.40	*1073*	*196.7*	*275.9*	*250.7*	*303.0*

[a]Numerals in italics refer to results from Risø. Last digit is uncertain.

Table 2. Structural parameters for orthorhombic $LaCo_{1-t}Cr_tO_3$ determined from PND.[a]

t	0.90	0.90	0.90	1.00	1.00
T/K	12	120	293	11	293
a/pm	546.07(4)	546.24(4)	546.97(5)	547.18(5)	548.28(5)
b/pm	773.73(10)	773.91(10)	775.29(11)	774.91(12)	776.92(10)
c/pm	550.26(7)	550.55(7)	551.18(6)	550.93(9)	552.17(6)
x_{La}	0.0216(6)	0.0208(6)	0.0182(6)	0.0241(6)	0.0186(6)
z_{La}	−0.0019(10)	−0.0008(10)	−0.0024(9)	−0.0013(13)	−0.0006(2)
x_{O1}	0.4936(9)	0.4941(9)	0.4951(9)	0.4937(10)	0.4933(9)
z_{O1}	0.0641(10)	0.0613(11)	0.0629(9)	0.0630(13)	0.0586(11)
x_{O2}	0.2262(7)	0.2271(7)	0.2286(7)	0.2243(8)	0.2284(7)
y_{O2}	0.5349(5)	0.5359(5)	0.5356(4)	0.5362(6)	0.5384(4)
z_{O2}	0.2259(7)	0.2269(7)	0.2283(7)	0.2255(8)	0.2253(6)

[a]Space group *Pnma*; La and O(1) in 4c, Co/Cr in 4b and O(2) in 8d. R_n ranges between 0.033 and 0.083, R_p between 0.056 and 0.080.

Table 4. Interatomic distances (in pm) for orthorhombic $LaCo_{1-t}Cr_tO_3$.[a]

t	0.90	0.90	0.90	1.00	1.00
T/K	12	120	293	11	293
Co/Cr–O1 (2×)	196.7	196.4	196.6	196.8	196.6
Co/Cr–O2 (2×)	196.3	196.5	196.4	197.4	196.2
Co/Cr–O2 (2×)	196.8	196.9	196.9	196.8	198.8
La–O1 (1×)	260.3	260.8	263.2	259.4	262.2
La–O1 (1×)	290.6	289.7	288.1	292.4	289.7
La–O1 (1×)	309.8	308.9	309.0	309.9	308.2
La–O1 (1×)	241.4	242.4	242.3	242.0	244.2
La–O2 (2×)	262.9	262.5	262.1	262.8	262.7
La–O2 (2×)	277.1	278.1	279.7	277.1	280.7
La–O2 (2×)	247.7	247.6	247.4	247.4	246.3
La–O2 (2×)	312.5	312.1	310.9	314.9	313.7

[a]Last digit is uncertain.

thus derived range between 3.07 and 3.22 for Co/Cr, between 2.77 and 2.85 for La, and −1.96 to −2.02 for O. Considering the many model uncertainties involved in the assessments, these bond valences may be said to match the expectations quite well. One possible explanation for the too large valences for Co/Cr, in particular at high Co-contents (where the discrepancy is largest), may be an incorrect choice of the bond-valence parameter for cobalt. The value compiled by Brese and O'Keeffe[51] does not distinguish between different electronic configurations for $3d^n$ cations, although their bond lengths differ, e.g., for LS and HS Co^{3+} by 6.5 pm.[53] Since one here obtains too large valences for cobalt, this may indicate that large emphasis has been put on high-spin cobalt in the compiled parameters in Ref. 51.

The structure data discussed in the literature for the suggested,[8] symmetry-reduced state ($R\bar{3}$) of $LaCoO_3$ differ considerably. The PXD data for $T > \sim 375$ K in Ref. 8 indicated an ordered distribution of LS and HS Co^{3+}, with an appreciable difference in the Co–O bond distance for the two types of cobalt atoms (171 vs. 217 pm at 400 K; average 194 pm). The PND study in Ref. 21, where oxygen positions were determined to a far higher accuracy, gave only indications of a reduced symmetry around 668 K, and even then, merely a slight difference in the Co–O bond distance (194.0 vs. 195.6 pm). However, conclusions from a more recent EXAFS study[34] were more in line with Ref. 8: ~166 vs. ~220 pm above 583 K. EXAFS is normally a powerful tool for exploring local surroundings, but the study in Ref. 34 appears to be hampered by statistics and too narrow a k-range. Moreover, bond valence considerations lead to improbable calculated valences, even if different parameters were chosen for LS and HS Co^{3+}. In summary, there seems to be no convincing structural support for the hypothesis of an ordered distribution of LS and HS Co^{3+} over the $LaCoO_3$ lattice.

With increasing chromium content, there is an increasing difference between the measured Co/Cr–O distance and the corresponding distance $[1/2(V/Z)^{1/3}]$ in a hypothetical, ideal cubic perovskite with the same volume V as the measured one. This reflects an increased tilting of the slightly distorted $(Co/Cr)O_6$ octahedra with increasing t, corresponding to a decreasing Co/Cr–O–Co/Cr angle (Fig. 1). The inset shows that the Co/Cr–O–Co/Cr angle increases with increasing temperature for $t = 0.40$, indicating that the structure strives slowly towards cubic.

Magnetic structure. The samples with $t = 0.00$, 0.10, 0.40, 0.90 and 1.00 were studied by PND at low temperatures in order to determine the magnetic order. No indication of magnetic orderering was found for $LaCoO_3$ and $LaCo_{0.90}Cr_{0.10}O_3$. These findings concur with earlier neutron diffraction studies[20,21] and are consistent with a d^6, $S = 0$ ground state for Co^{3+}.

On going through the intermediate and high-temperature range, $LaCoO_3$ is variously believed to be in a mixed LS/HS,[4,8,9,11–16,22,23,29,31] IS,[12,16] mixed IS/HS[16] or HS[4,8,9,11–16,22,23,29,31] state. Asai *et al.*[22,23] found clear indications for spin changes in the paramagnetic scattering below 300 K. For that reason the temperature

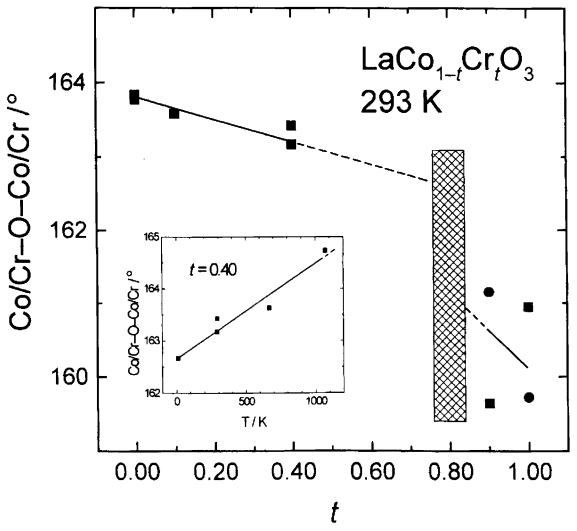

Fig. 1. Variation in the octahedral angle Co/Cr–O–Co/Cr with t in $LaCo_{1-t}Cr_tO_3$ and temperature for $t = 0.40$ (inset). The line in the orthorhombic region represents weighted average. Estimated error limits are about twice the size of the symbols.

dependence of the diffuse scattering contribution to the background at low angles ($4.0 \leqslant 2\Theta \leqslant 4.5°$) was also measured between 9 and 300 K in the present study. However, no significant changes were observed, viz. the paramagnetic scattering contribution for the present sample was roughly unchanged between 9 and 300 K. An effect of the same order as we found for the conversion of LS to HS for $MnAs_{1-x}P_x$[54] can definitely be ruled out. This result does not necessarily contradict the findings by polarized neutron paramagnetic scattering since Asai *et al.*[22,23] do not specify the extent of the spin conversion.

For rhombohedral $LaCo_{0.60}Cr_{0.40}O_3$, the observation of two additional, partly overlapping reflections, (100) and (111), in the PND pattern at 11 K (Fig. 2) proves the occurrence of long-range magnetic order. A uniaxial description of the magnetic structure was adopted in the Rietveld refinements (program MPROF[46]). Since the magnetic susceptibility data show that the sample is in a ferrimagnetic state, ferromagnetic components were introduced in the initial calculations. However, the ferromagnetic contributions turned out to be well below the detection limit and hence not included in the final refinements. According to the PND data, the magnetic structure is of the *G* type. The ordered magnetic moment at 11 K is $\mu_{AF} = 1.22(6)\ \mu_B$, with parallel and perpendicular components with respect to the unique [001] axis (hexagonal setting) of 0.74(9) and 0.97(4) μ_B, respectively. The Néel temperature was determined as $T_N = 100 \pm 15$ K from the temperature variation of the integrated intensity of the partly overlapping (100) and (111) reflections.

For orthorhombic $LaCrO_3$ and $LaCo_{0.10}Cr_{0.90}O_3$, several additional magnetic reflections are observed at 11 K. For $LaCrO_3$, G_x ordering is reported;[41] for Ca-substituted variants with a small additional A_z contribution.[42] The modes G_x, C_y, A_z belong to the same irreducible representation and were included in the refinements. There was no indication for G_y or G_z components. The as-determined magnetic moments are given in Table 5, but the values for the C_y and A_z components are so small that they should be considered insignificant. The magnetic structures for rhombohedral ($t = 0.40$) and orthorhombic ($t = 0.90$ and 1.00) $LaCo_{1-t}Cr_tO_3$ are shown in Fig. 3. The calculated fits of the experimental data to the crystal and magnetic structure model are good, as seen from Fig. 4 for $LaCo_{0.10}Cr_{0.90}O_3$ and the *R*-factors in Tables 2 and 5. The Néel temperatures for $t = 0.90$ and 1.00 were determined from the temperature dependence of the integrated intensity of the magnetic (011)/(110) peak (Fig. 5); $T_N = 272 \pm 5$ K for $t = 0.90$ and $T_N = 297 \pm 5$ K for $t = 1.00$.

Low-temperature magnetic susceptibility for $LaCo_{1-t}Cr_tO_3$. Magnetic susceptibility data were measured for zero-field-cooled (ZFC) and field-cooled (FC) samples throughout the $LaCo_{1-t}Cr_tO_3$ solid-solution range. The results are conveniently grouped in the two composition intervals, $0.10 \leqslant t \leqslant 0.30$ and $0.40 \leqslant t \leqslant 1.00$. Data for the temperature interval 300–1000 K and for $LaCoO_3$ are considered separately below. Inverse magnetic susceptibility versus temperature curves are shown for $t = 0.10$, 0.20 and 0.30 in Fig. 6. No indications are found for magnetic order, and no field- or history-dependence is

Table 5. Refined magnetic moments (in μ_B) for $LaCo_{1-t}Cr_tO_3$.[a]

t	*T*/K	G_x	C_y	A_z
0.90	12	2.17(2)	0.24(9)	0.19(6)
0.90	120	2.05(2)	0.18(12)	0.26(4)
1.00	11	2.36(2)	0.10(11)	0.30(4)

[a] R_m ranges between 0.110 and 0.136. Calculated standard deviations in parantheses.

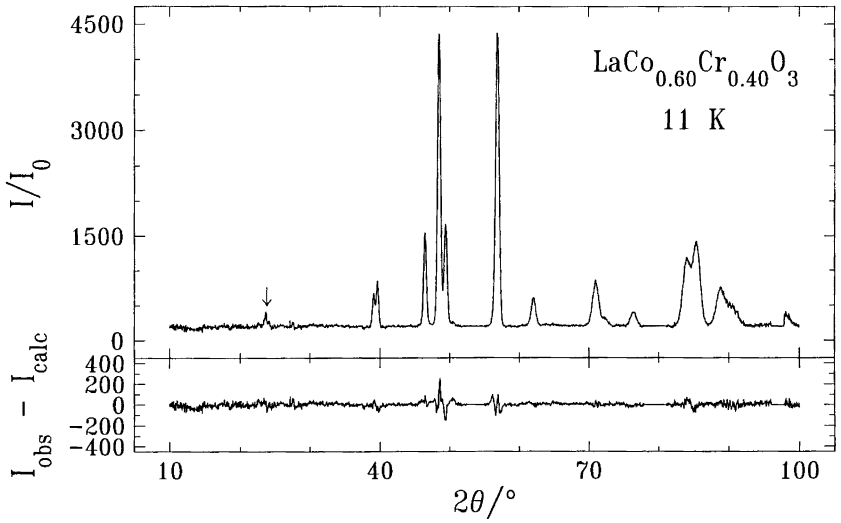

Fig. 2. Observed and difference PND diagrams for $LaCo_{0.60}Cr_{0.40}O_3$ at 11 K. The partly overlapping magnetic reflections 100 and 111 are marked with an arrow, whereas reflections with weaker magnetic contributions are not indicated.

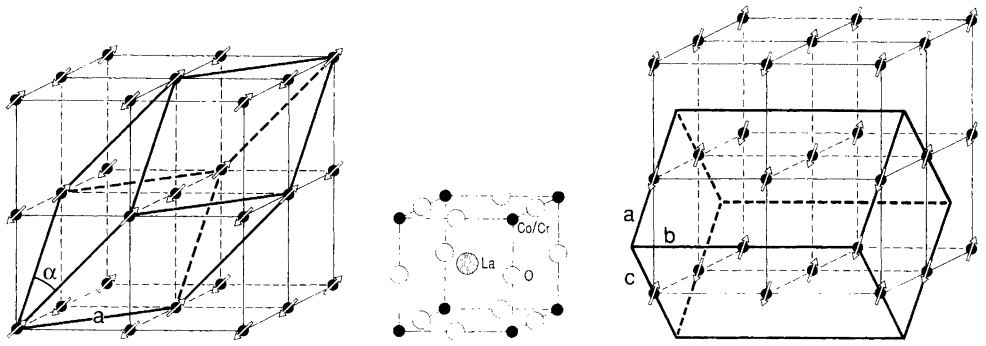

Fig. 3. Magnetic structures for rhombohedral (t=0.40, left) and orthorhombic (t=0.90 and 1.00, right) $LaCo_{1-t}Cr_tO_3$. The atomic arrangement of the idealized, cubic perovskite-type structure is shown in the middle.

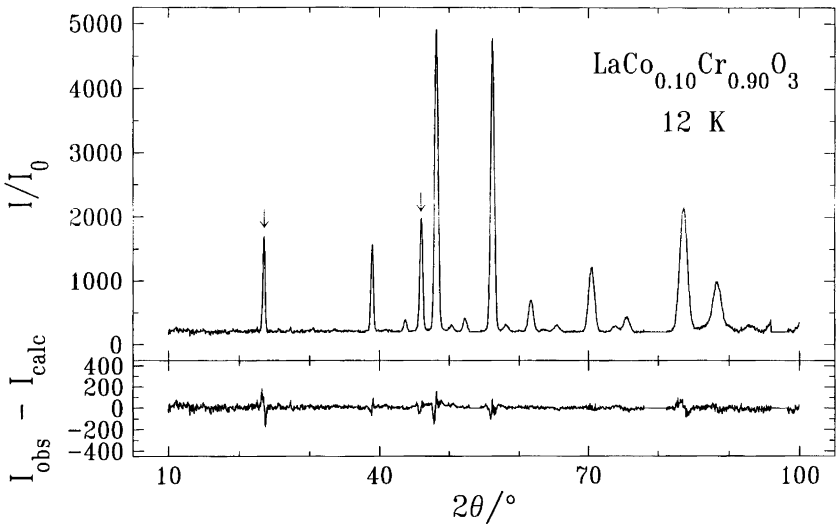

Fig. 4. Observed and difference PND diagrams for $LaCo_{0.10}Cr_{0.90}O_3$ at 12 K. Reflections with significant magnetic contributions are marked with arrows.

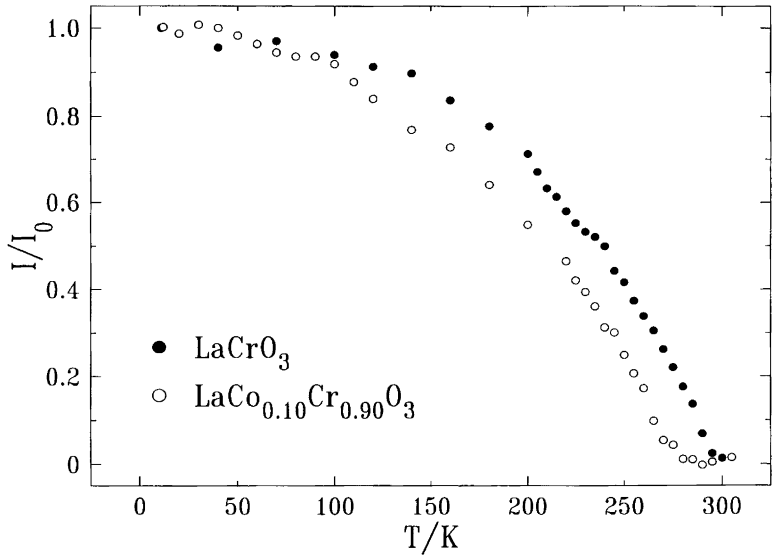

Fig. 5. Integrated intensities for the magnetic 011/110 reflection versus temperature for $LaCo_{1-t}Cr_tO_3$ with t=0.90 and 1.00.

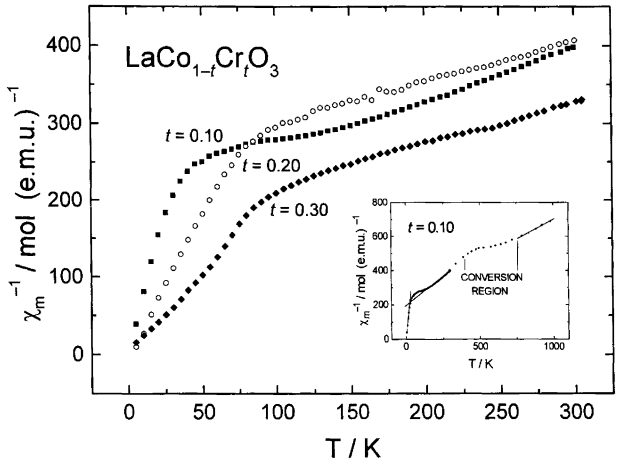

Fig. 6. Inverse magnetic susceptibility (ZFC) versus temperature (5–300 K) for $LaCo_{1-t}Cr_tO_3$ with $t=0.10$, 0.20 and 0.30. The inset shows $\chi^{-1}(T)$ for $t=0.10$ (5–1000 K). Curie–Weiss fitted regions are indicated. Data for $T>300$ K in the inset refer to Faraday balance measurements.

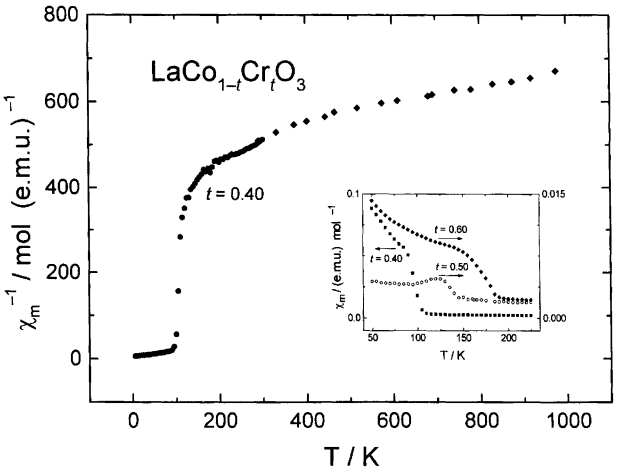

Fig. 7. Inverse magnetic susceptibility (ZFC) versus temperature (5–1000 K) for $LaCo_{0.60}Cr_{0.40}O_3$. ◆ refers to Faraday balance measurements. The inset shows $\chi(T)$ for $LaCo_{1-t}Cr_tO_3$ with $t=0.40$, 0.50 and 0.60 (50–225 K).

found for $H\leqslant 5$ kOe. The Curie–Weiss law is fulfilled at the lowest temperatures, effective paramagnetic moments being 1.05, 1.46 and 1.9μ_B for $t=0.10$, 0.20 and 0.30, respectively. The Weiss constant (Θ) is zero within the experimental uncertainty. The size of these moments corresponds reasonably well with expected values for diluted, non-interacting Cr^{3+} ions in a matrix of LS Co^{3+}. The percolation limit for magnetic ordering (ruled by chromium) on the Co/Cr sublattice appears to be $t\approx 0.35$. At temperatures between some 30 and 150 K, $\chi^{-1}(T)$ signals a transition to a different paramagnetic state, above which the Curie–Weiss law is again obeyed, with significantly larger effective paramagnetic moments (3.47, 3.95 and 3.96 μ_B for $t=0.10$, 0.20 and 0.30, respectively) and large negative Θ-values (−294, −491 and −338 K, respectively). A second change in paramagnetic properties occurs above ca. 400 K; see inset to Fig. 6 for $t=0.10$ and *vide infra*.

The rhombohedral samples with $0.40\leqslant t\leqslant 0.60$ as well as the orthorhombic samples with $0.70\leqslant t\leqslant 1.00$ are magnetically ordered at low temperatures (*vide supra*). The temperature dependences of the magnetic susceptibility for $t=0.40$, 0.50 and 0.60 under ZFC conditions are shown in the inset to Fig. 7. The samples with $t=0.40$ and 0.60 seem to be ferromagnetic, but according to PND, the ferromagnetic component is small and escapes detection. For samples with antiferromagnetic behaviour, a weak additional ferromagnetic component develops under FC conditions, as shown for $t=0.70$ in Fig. 8. This ferromagnetic contribution may possibly arise from double exchange interactions between cations in different oxidation states, most likely between Cr^{3+} and Cr^{4+}, the latter introduced into the samples from divalent cation impurities in the starting materials. It may also reflect a spin-turning of a slightly canted initial antiferromagnetic structure, similar to that found for $LaCrO_3$.[41]

The inverse magnetic susceptibility versus temperature curve for $LaCo_{0.30}Cr_{0.70}O_3$ in Fig. 8 is representative for the orthorhombic region $0.70\leqslant t\leqslant 1.00$ for $T\sim 200$ K. The minimum in $\chi^{-1}(T)$ at ca. 200 K in the 0.100 kOe ZFC curve in Fig. 8 reflects T_N. For most of the samples in this region, there occurs another, rather weak minimum between 55 and 85 K, most pronounced for $t=0.90$. However, no changes in the magnetic structure could be observed by PND, implying that only minor perturbations can be involved.

The ZFC $LaCrO_3$ sample shows antiferromagnetic behaviour (Fig. 9), but even for this composition there is a distinct difference between the ZFC and FC data. The weak parasitic ferromagnetism reflected below ~300 K in Fig. 9 is again either caused by divalent cation impurities or spin-turning.

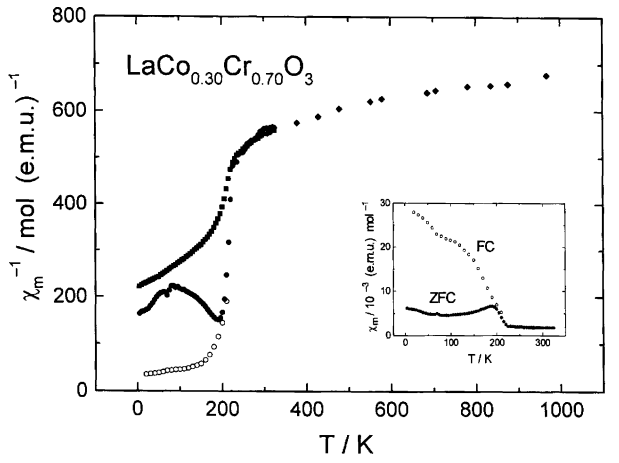

Fig. 8. Temperature dependence (5–1000 K) of inverse magnetic susceptibility for $LaCo_{0.30}Cr_{0.70}O_3$. ■, ZFC, 50 kOe; ●, ZFC, 0.100 kOe; ○, FC, 0.100 kOe, measurements on decreasing temperature; ◆, Faraday balance measurements.

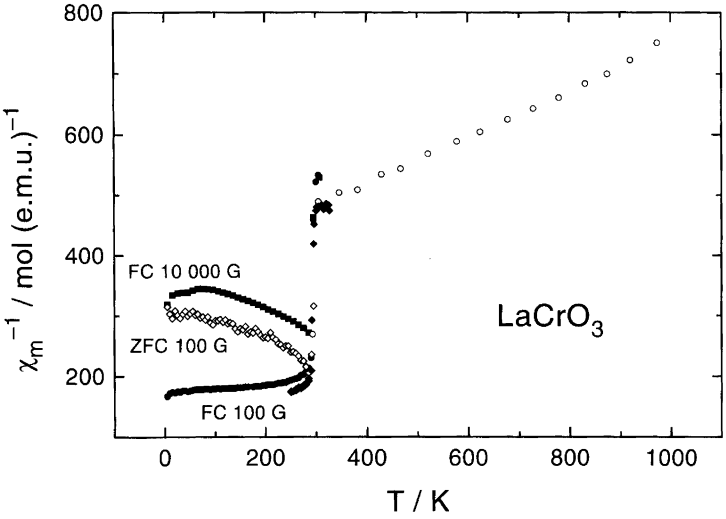

Fig. 9. Temperature dependence (5–1000 K) of inverse magnetic susceptibility for $LaCrO_3$. FC measurements performed with decreasing temperature.

High-temperature magnetic susceptibility for $LaCo_{1-t}Cr_tO_3$. Inverse magnetic susceptibility data for $LaCo_{1-t}Cr_tO_3$ between 300 and 1000 K are shown in Fig. 10. The two Curie–Weiss regimes described for $LaCoO_3$ become less distinct when the Cr content increases, and the range for the so-called moment conversion seems to shift to higher temperatures. The conversion phenomenon hence extends into the solid-solution phase. The deviation from linear of the $\chi^{-1}(T)$ plots varies with t, and it becomes gradually less pronounced with increasing Cr content. Thus the estimation of the width of the conversion region as well as the magnetic moments before and after the conversion becomes increasingly more difficult. For certain compositions, the conversion is perhaps not even completed at the highest temperatures (1000 K). If so, simple analyses of the slopes of the $\chi^{-1}(T)$ curves would give too large magnetic moments. For the high-temperature regime, the deduced paramagnetic moment increases from 4.0 μ_B for $LaCoO_3$ to a maximum of 6.7 μ_B for $LaCo_{0.30}Cr_{0.70}O_3$, and then decreases rather steeply for $0.80 \leqslant t \leqslant 1.00$ towards 4.5 μ_B for $LaCrO_3$.The latter moment is somewhat above the spin-only value, but is in agreement with literature data for $LaCrO_3$.[41]

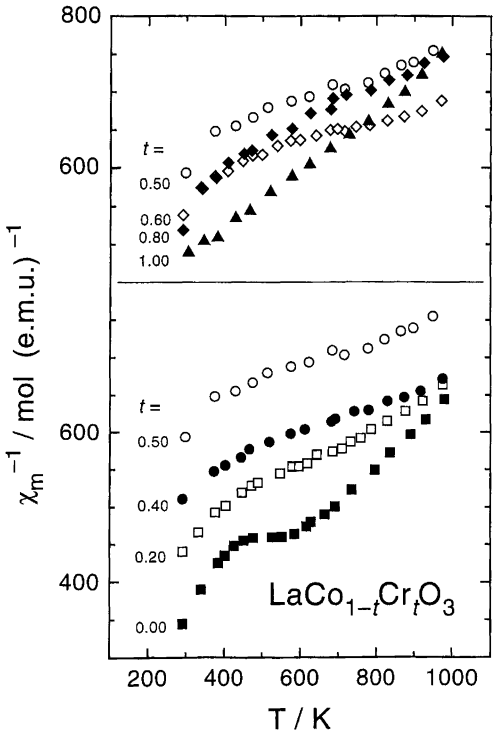

Fig. 10. Temperature dependence (300–1000 K) of Faraday balance inverse magnetic susceptibilty for $LaCo_{1-t}Cr_tO_3$.

Magnetic susceptibility for $LaCoO_3$. The low-temperature ($T < 100$ K) magnetic behaviour of $LaCoO_3$ is very complex. In the literature, rather few, independent magnetic susceptibilty data are available in spite of the apparently numerous experiments which have been carried out. According to the criteria of PXD and DTA, the present $LaCoO_3$ samples showed no indications of any impurities. In particular, no endothermic peak in DTA corresponding to decomposition of Co_3O_4 at 1210 K was observed. According to Señaris-Rodriguez and Goodenough,[14] the sample should hence be of good quality. The inverse susceptibility data in Fig. 11 ($H =$ 50 kOe for $T < 300$ K, SQUID; $H = 2$–8 kOe for $T > 300$ K, Faraday) nicely reproduce the $\chi^{-1}(T)$ relationship reported by Señaris-Rodriguez and Goodenough (10 kOe for $T < 380$ K, 5 kOe for $T > 380$ K, SQUID).[14]

There are significant differences in some of the magnetic susceptibility curves collected for different samples of $LaCoO_3$, all of which appear to be single phase according to PXD (and PND for one sample), with identical unit-cell dimensions (within one standard deviation). Nevertheless, these samples represent different

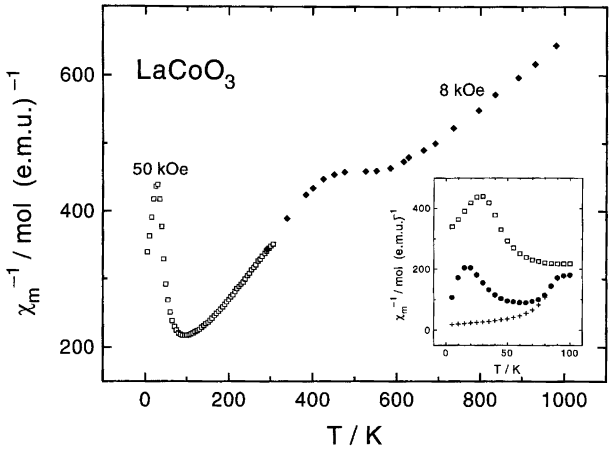

Fig. 11. Inverse magnetic susceptibility versus temperature (5–320 K, increasing temperature, ZFC, 50 kOe, SQUID; 300–1000 K, 2–8 kOe, Faraday) for $LaCoO_3$. In the inset, + refers to FC, 0.500 kOe, ● to ZFC, 0.500 kOe and □ to ZFC, 50 kOe.

batches, synthesized according to the same recipe, but with individual temperature and oxygen equilibration treatments. It seems reasonable to claim that the magnetic properties of $LaCoO_3$ are extremely sensitive to modest compositional changes, possibly introduced by, e.g., divalent cation (M) impurities ($La_{1-x}M_xCoO_3$) and/or by oxygen defects ($La_{1-x}M_xCoO_{3-\delta}$). The non-stoichiometry depends on both the temperature and the oxygen partial pressure, and the annealing times available are insufficient for obtaining the real equilibrium state at room temperature. The sample therefore maintains a sort of frozen-in state, characteristic of some unspecified, higher temperature. However, an annoying aspect in the lack of reproducibility is that the source of the 'impurity' has not yet been disclosed. The low-temperature ($T<100$ K) magnetisation behaviour of $LaCoO_3$ is clearly field dependent, and depends to some extent on the entire measurement history experienced by a given sample. As seen from the inset to Fig. 11, below some 100 K, FC samples obtain a substantially larger magnetic susceptibility than ZFC samples. In the same temperature range, the magnetic susceptibility shows strong field dependence (inset to Fig. 11), indicating ferromagnetic interactions. In low to moderate fields, there exists a broad minimum in $\chi^{-1}(T)$ around 70 K. In high fields, above some 10 kOe, the minimum disappears. On $1/H$ extrapolation of the saturation magnetisation at 10 K to infinite field strength one obtains 0.41 e.m.u. g^{-1}, which corresponds to 0.018 μ_B per Co atom. If this moment is ascribed to Co^{4+}, this would involve 0.3% of the cobalt atoms. Already at a substitution level of 1% Cr ($LaCo_{0.99}Cr_{0.01}O_3$), the pronounced field dependence for $T\sim100$ K has disappeared, while the maximum in $\chi^{-1}(T)$ at ~35 K is maintained. This maximum decreases rapidly with increasing chromium substitution and is already reduced to about half its original size for $LaCo_{0.97}Cr_{0.03}O_3$. Above ~100 K the $\chi^{-1}(T)$ curves for $t=0.01$ and 0.03 nearly overlap that of $LaCoO_3$. There seems to be a certain, but much weaker field dependence in $\chi^{-1}(T)$ above ~100 K. At 5 K the $M(H)$ curve for $LaCoO_3$ exhibits a small hysteresis, as also reported by Menyuk *et al.*[7]

Above ~100 K, $\chi^{-1}(T)$ obeys the Curie–Weiss law; in the temperature range ~150–~400 K with $\mu_p=3.17(10)\mu_B$ and $\Theta=-89(5)$ K and for ~650–1000 K, $\mu_p=4.04(6)\mu_B$ and $\Theta=-79(3)$ K. The thus deduced apparent change in moment between ~400 and ~650 K (cf. Fig. 11) agrees well with data reported in the literature.[4,6,8,9,11,14–16]

Discussion

The low-temperature anomalous magnetic susceptibility of $LaCoO_3$, $T<100$ K. There exist at least three separate, experimental indications for an $S=0$ ground state of cobalt in $LaCoO_3$ at 0 K. First, polarized neutron scattering data for a single crystal show no paramagnetic intensity contribution at 10 K.[22,23] Second, NMR data (Knight shifts for ^{59}Co and ^{139}La) clearly indicate a diamagnetic ground state.[13] Third, the present low-temperature magnetic susceptibility data for $LaCo_{1-t}Cr_tO_3$ with $0.10\leqslant t\leqslant0.30$, correspond to just slightly lower paramagnetic moments than what would be expected for diluted, non-interacting Cr^{3+} ions in a diamagnetic matrix. Additional support comes from recent electronic band-structure calculations[37] and, more indirectly, from heat capacity measurements.[32]

The lack of magnetic long-range order seen by PND at low temperature is, on the other hand, no proof for an $S=0$ ground state. For comparison, no magnetic long-range order is found at low temperature for the related $LaMnO_{3.15}$ phase, which has almost the same atomic arrangement and exhibits large paramagnetic moments at high temperatures. For $LaMnO_{3.15}$ this probably originates from frustration of positive and negative interactions, whereas other stoichiometries, e.g. $LaMnO_{3.00}$, exhibit large ordered moments.[55]

The magnetic susceptibility data for $LaCoO_3$ are not without further ado compatible with an $S=0$ ground state at 0 K. The magnetic susceptibility below 100 K is positive, rather large and shows field dependence. Inclusion of a ferromagnetic phase, intimately related to the $LaCoO_3$ perovskite, has been reported, e.g., by Menyuk *et al.*[7] and Asai *et al.*[23] for powder as well as single crystal samples. Asai *et al.* found by neutron diffraction on a $LaCoO_3$ single crystal additional magnetic peaks with intensities that vanished first around 250–300 K, and which they ascribed to a ferromagnetic impurity. The ferromagnetic feature which has been observed below 100 K in this study may have the same origin, but it is possible that there are different sources for the various field effects found by different research groups. It is noteworthy that the ferromagnetic features are already removed at a Cr substitution level of $t=0.03$. It is also possible (*vide supra*) that our lanthanum cobalt

oxide sample, as well as those of other researchers, in reality should be described as $(La_{1-x}M_x^{2+})CoO_{3-\delta}$ (M in sub-percent amounts). Under oxidizing conditions there are reasons to expect $\delta=0$, and the Co^{4+} species thus implied may be imagined to cluster and give rise to field-dependent behaviour below a certain temperature (in this case 100 K). At very high temperatures and/or under reducing conditions, Co^{2+} occurs as a compensation for the intrinsic formation of oxygen vacancies. It is hence possible that Co^{2+} exists in single crystals grown from the melt if the thermal equilibration in oxygen has been insufficient. Upon Cr substitution, TPR and XPS data[2] indicate that higher valent chromium is present at the surface of the $LaCo_{1-t}Cr_tO_3$ particles. For $(La_{1-x}M_x^{2+})Co_{1-t}Cr_tO_{3-\delta}$ it is feasible that, say, Cr^{4+} is formed instead of Co^{4+}. The fact that there is an increasing tendency to form ferromagnetic clusters in the $La_{1-x}Sr_xCoO_3$ phase with increasing x also lends support to the divalent impurity hypothesis.[42]

The directly opposite attitude would be to maintain that the field-strength-dependent magnetic susceptibility below 100 K after all is an intrinsic property of $LaCoO_3$. On deconvolution of the c_p curve into contributions from different sources, Stølen *et al.*[32] found a small, broad hump in the low temperature region ($20<T<100$ K), which they tentatively attribute to a transition from the Co^{3+}, LS ground state at $T=0$ K to a 'stable' Co^{3+}, IS state with additional contribution originating from electron energy level splitting through spin–orbit coupling. It is possible that the IS state is orbital-ordered,[37,56] perhaps with weak ferromagnetic interactions,[23] which could explain some of the present findings. The electronic band schemes involved in this picture are accordingly rather complex [significant L–S coupling, at least three states close in energy ($^1A_{1g}$, $^3T_{1g}$ and $^5T_{2g}$) with additional trigonal distortion of the octahedral electric field and possibly with Zeeman effects in strong magnetic fields], and certainly more faceted than the two-level scheme used by Naiman *et al.*[5] to discuss the temperature variation of the magnetic susceptibility of (single crystal) $LaCoO_3$. Nevertheless, the model of Naiman *et al.*[5] (see also Ref. 12) is able to account for a number of the observed features in $\chi^{-1}(T)$. As an aspect of interest for the question under consideration, Naiman *et al.* specifically point out that 'the susceptibility could be magnetic-field-dependent'. All in all, the present authors tend to favour the intrinsic explanation.

Spin state conversions at and above 100 K. The pronounced field dependence of the magnetic susceptibility of $LaCoO_3$ ceases at $\sim$100 K. According to the above intrinsic interpretation, this would mean that the majority of the electrons that can be perturbed by a magnetic field are already fully perturbed at 100 K. The removal of the dramatic magnetic field effect already at the substitution level $t=0.01$ supports the existence of closely spaced energy levels which are easily modified by small amounts of paramagnetic substituents. The low-temperature anomaly inferred from the deconvoluted c_p curve of Stølen *et al.*[32] also has a maximum at 100 K. The fact that this anomaly apparently continues above 100 K may be accounted for by recalling that the thermodynamic measurements are performed without a magnetic field.

In terms of the divalent impurity concept, 100 K merely represents the 'Curie' temperature of the ferromagnetic clusters (*vide supra*). For temperatures above the freezing (blocking) temperature of these clusters, one could envisage that superparamagnetic clusters, with Co^{4+} and/or Co^{3+} as near-neighbours to the (divalent) impurity, can give rise to large magnetic moments, and account for the apparent Curie–Weiss law dependence. In $La_{1-x}Sr_xCoO_3$ and $LaCo_{1-t}Mn_tO_3$, giant magnetic moments corresponding to spin quantum numbers up to 16 have been reported.[12,15] However, the present data show no smooth M versus $\log(H/T)$ dependence, so superparamagnetism is not likely in the interval $100\leqslant T\leqslant 300$ K. One is accordingly faced with the only possibility that the origin of the paramagnetism of $LaCoO_3$ above ca. 100 K is a spin conversion from LS to a higher spin state. The spin conversion is gradual and observable already at 20 K,[32] but was not observed by XAS above 80 K.[26] It was, however, detected by Co $3p$–$3d$ resonant photoemission spectroscopy, where significant changes were found between 20 and 80 K.[57] Recent theoretical calculations suggest that an insulating LS state is the ground state at low temperature, with two IS states at somewhat higher energies, and a HS state at significantly higher energy.[37] The earlier assumed direct LS–HS conversion is moreover not compatible with ^{17}O, ^{59}Co and ^{139}La NMR Knight shift data collected below 300 K.[58] Additional evidence for a gradual conversion from LS to an (orbital-ordered) IS state around 100 K comes from the variation of the Co–O–Co stretching mode with increasing temperature.[56] In conclusion, all evidence suggests that the IS state really exists.

The as-measured c_p data set[32] shows a pronounced peak with a maximum at $\sim$530 K, which reflects the insulator–metal conversion and the thus associated rearrangement of the electronic band structure. Korotin et al.[37] suggest that the insulator–metal transition could be associated with the disappearance of orbital ordering in the IS state. This view is not supported by the recent experimental and theoretical study of $LaCoO_3$ excitation spectra.[59] However, in the latter work, the structural distortions were not taken into account when the spectra were theoretically simulated. It is more or less generally accepted that distortions from the ideal, cubic perovskite-type structure are of importance for the insulator–metal transition; in fact, the transition temperature increases with decreasing Co–O–Co angle in the $RCoO_3$ (R = La, Pr, Nd, Sm, Eu and Gd) series.[60] Furthermore, it is documented that the actual structure must be taken into account in order to obtain a satisfactory agreement between calculated and experimental X-ray absorption spectra.[61] Although many aspects of this transition must still be regarded as open, it is clearly energetically

stronger than the transition centered at ~100 K, and it actually starts before the first process is terminated.[32] It is therefore natural to expect that the $\chi^{-1}(T)$ curve should exhibit a complex, composite behaviour. In this situation, little significance should be attached to the μ_P and Θ_P values which have been extracted from the apparent Curie–Weiss regions for $LaCoO_3$ in Fig. 11. In fact, more or less the entire Co-rich part of the $LaCo_{1-t}Cr_tO_3$ phase is in the same position, and for this reason we hesitate to specify μ_P- and Θ-values. The spin conversion feature of the $LaCo_{1-t}Cr_tO_3$ phase is attempted summarized in the tentative phase diagram in Fig. 12. The possibility for dynamic or static ordering of various cobalt and chromium 'spin species' has been considered, but we found no conclusive support for any such ordering at and below 300 K (1100 K for $t=0.40$). However, such spin and/or charge ordering does appear possible, cf. the ordering of different Co species in $Ca_3Co_2O_6$[62] and of Mn species in $LaCaMn_2O_6$.[63]

There is a relevant question regarding the type and amount of Co^{3+} which is not in the LS state at, e.g., 300 K. The literature gives no definite answer to this question. The question can to some extent be approached by considering the structural data for $LaCo_{1-t}Cr_tO_3$. The variation in the Co/Cr–O distance as a function of composition (which matches the findings for $NdCo_{1-t}Cr_tO_3$[64]) shows that cobalt here has a much smaller size than Cr^{3+}. Considering the ionic radii for CN=6, $r(Cr^{3+})=61.5$, $r(Co^{3+},HS)=61$ and $r(Co^{3+},LS)=54.5$ pm,[53] the interatomic distances in Table 3 indicate that cobalt is closer to LS than HS at 298 K. For $LaCo_{1-t}Cr_tO_3$, the difference in unit-cell volume between the end members amounts to $\Delta V = V(LaCrO_3)/Z - V(LaCoO_3)/Z = 2.6\times10^6$ pm^3 at 298 K and $\Delta V = 3.4\times10^6$ pm^3 at 10 K. For the corresponding (orthorhombic) $NdCo_{1-t}Cr_tO_3$ phase, $\Delta V = 3.4\times10^6$ pm^3 at 298 K.[64] This indicates that cobalt has the same (low-)spin state at low temperature in $LaCoO_3$ and $NdCoO_3$. At higher temperatures, ΔV for $LaCo_{1-t}Cr_tO_3$ is much reduced and has become 0.5×10^6 pm^3 at 1033 K. The progressive evolution in ΔV for $LaCo_{1-t}Cr_tO_3$ as a function of t and T (differences in structural arrangements taken into account) may be taken as an indication for the proposed 'spin' conversion region in Fig. 12. Additional support for the spin conversion comes from the temperature variation in the Co–O distance in $LaCoO_3$ reported by Asai *et al.*[16] Furthermore, the anomalous large thermal expansion for $LaCo_{1-t}Cr_tO_3$ is also indicative of 'spin' conversion processes which occur over large temperature intervals. For $0.00 \leqslant t < \sim 0.65$, $\alpha_V \approx 6.5\times10^{-5}$ K^{-1}, whereas for $\sim 0.65 \leqslant t \leqslant 1.00$, α_V decreases linearly to 2×10^{-5} K^{-1}. The anomaly in α_V for $LaCoO_3$[1] in the temperature interval of the inferred semiconductor (IS) to metal (IS or HS) transition diminishes up to a substitution level of $t=0.60$. Thus, we see concurrent changes in the spin state, volume expansion and electronic band structure.

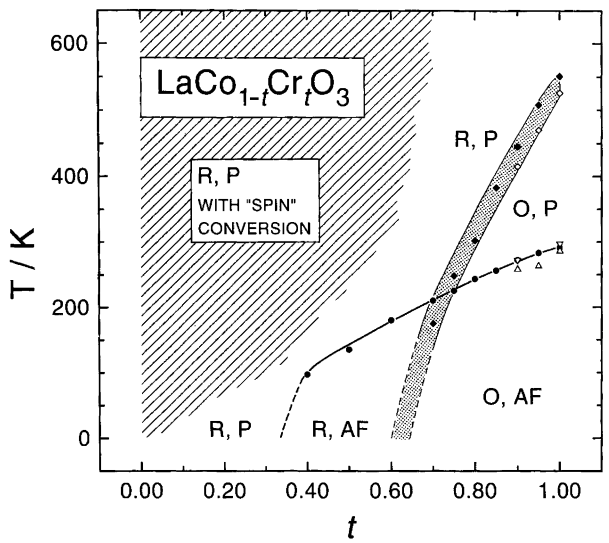

Fig. 12. Tentative structural and magnetic phase diagram for $LaCo_{1-t}Cr_tO_3$. Abbreviations: R rhombohedral ($LaAlO_3$ type), O orthorhombic ($GdFeO_3$ type), AF antiferromagnetic, P paramagnetic. Symbols: △ and ◇ DSC, ▽ PND, ◆ PXD, ● magnetic susceptibility.

Acknowledgements. The possibility to collect powder neutron diffraction data at Risø, Roskilde, Denmark is gratefully acknowledged. The project has obtained support from The Research Council of Norway.

References

1. Gilbu, B., Fjellvåg, H. and Kjekshus, A. *Acta Chem. Scand. 48* (1994) 37.
2. Tilset, B. Gilbu, Fjellvåg, H. and Kjekshus, A. *J. Solid State Chem. 119* (1995) 271.
3. Tilset, B. Gilbu, Fjellvåg, H., Kjekshus, A., Slagtern, Å. and Dahl, I. *Appl. Catal., Part A 147* (1996) 189.
4. Heikes, R. R., Miller, R. C. and Mazelsky, R. *Physica 30* (1964) 1600.
5. Naiman, C. S., Gilmore, R., DiBartolo, B., Linz, A. and Santoro, R. *J. Appl. Phys. 36* (1965) 1044.
6. Jonker, G. H. *J. Appl. Phys. 37* (1966) 1424.
7. Menyuk, N., Dwight K. and Raccah, P. M. *J. Phys. Chem. Solids 28* (1967) 549.
8. Raccah, P. M. and Goodenough, J. B. *Phys. Rev. 155* (1967) 932.
9. Bhide, V. G., Rajoria, D. S., Rao, G. R. and Rao, C. N. R. *Phys. Rev. B 6* (1972) 1021.
10. Ramadass, N., Gopalakrishnan, J. and Sastri, M. V. C. *J. Less-Common Metals 65* (1979) 129.
11. Madhusudan, W. H., Vasanthacharya, N. Y. and Ganguly, P. *Ind. J. Chem. 19A* (1980) 1037.
12. Vasanthacharya, N. Y. and Ganguly, P. *Bull. Mater. Sci. 5* (1983) 307.
13. Itoh, M., Sugahara, M., Natori, I. and Motoya, K. *J. Phys. Soc. Jpn. 64* (1995) 3967.
14. Señarís-Rodríguez, M. A. and Goodenough, J. B. *J. Solid State Chem. 116* (1995) 224.
15. Yamaguchi, S., Okimoto, Y., Taniguchi, H. and Tokura, Y. *Phys. Rev. B 53* (1996) R2926.
16. Asai, K., Yoneda, A., Yokokura, O., Tranquada, J. M., Shirane, G. and Kohn, K. *Personal communication to Ref. 32.*

17. Saitoh, T., Mizokawa, T., Fujimori, A., Abbate, M., Takeda, T. and Takano, M. *Phys. Rev. B 55* (1997) 4257.
18. Thornton, G., Tofield, B. C. and Williams, D. E. *Solid State Commun. 44* (1982) 1213.
19. Thornton, G., Morrison, F. C., Partington, S., Tofield, B. C. and Williams, D. E. *J. Phys. C 21* (1988) 2871.
20. Koehler, W. C. and Wollan, E. O. *J. Phys. Chem. Solids 2* (1957)100.
21. Thornton, G., Tofield, B. C. and Hewat, A. W. *J. Solid State Chem. 61* (1986) 301.
22. Asai, K., Gehring, P., Chou, H. and Shirane, G. *Phys. Rev. B 40* (1989) 10982 .
23. Asai, K., Yokokura, O., Nishimori, N., Chou, H., Tranquada, J. M., Shirane, G., Higuchi, S., Okajima, Y. and Kohn, K. *Phys. Rev. B 50* (1994) 3025.
24. Thornton, G., Owen, I. W. and Diakun, G. P. *J. Phys. Condens. Matter 3* (1991) 417.
25. Sarma, D. D., Chainani, A., Cimino, R., Sen, P., Carbone, C., Mathew, M. and Gudat, W. *Europhys. Lett. 19* (1992) 513.
26. Abbate, M., Fuggle, J. C., Fujimori, A., Tjeng, L. H., Chen, C. T., Potze, R., Sawatzky, G. A., Eisaki, H. and Uchida, S. *Phys. Rev. B 47* (1993) 16124.
27. Abbate, M., Potze, R., Sawatzky, G. A. and Fujimori, A. *Phys. Rev. B 49* (1994) 7210.
28. Richter, L., Bader, S. D. and Brodsky, M. B. *Phys. Rev. B 22* (1980) 3059.
29. Lam, D. J., Veal, B. W. and Ellis, D. E. *Phys. Rev. B 22* (1980) 5730.
30. Main, I. G., Robins, G. A. and Demazeau, G. *J. Phys. C 14* (1981) 3633.
31. Barman, S. R. and Sarma, D. D. *Phys. Rev. B 49* (1994) 13979.
32. Stølen, S., Grønvold, F., Brinks, H., Atake, T. and Mori, H. *Phys. Rev. B 55* (1997) 14103.
33. Orchard, A. F. and Thornton, G. *J. Electron Spectrosc. Relat. Phenom. 22* (1981) 277.
34. Arunarkavalli, T., Kulkarni G. U. and Rao, C. N. R. *J. Solid State Chem. 107* (1993) 299.
35. Marx, R. and Happ, H. *Phys. Stat. Sol. (b) 67* (1975) 181.
36. Takahashi, H., Munakata, F. and Yamanaka, M. *Phys. Rev. B 53* (1996) 3731.
37. Korotin, M. A., Ezhov, S. Y., Solovyev, I. V., Anisimov, V. I., Khomskii, D. I. and Sawatzky, G. A. *Phys. Rev. B 54* (1996) 5309.
38. Mizokawa, T. and Fujimori, A. *Phys. Rev. B 54* (1996) 5368.
39. Rao, G. V. S., Wanklyn, G. M. and Rao, C. N. R. *J. Phys. Chem. Solids 32* (1971) 345.
40. Tripathi, A. K. and Lal, H. B. *J. Mater. Sci. 17* (1982) 1595.
41. Bertaut, E. F., Mareschal, J., de Vries, G., Aléonard, R., Pauthenet, R., Rebouillat, J. P. and Zarubicka, V. *IEEE Trans. Magn. 2* (1966) 453.
42. Sakai, N., Fjellvåg, H. and Hauback, B. C. *J. Solid State Chem. 121* (1996) 202.
43. Tolochko, S. P., Kononyuk, I. F., Zonov, Yu. G. and Ivashkevich, L. S. *Izv. Akad. Nauk SSSR, Neorg. Mater. 23* (1987) 829. [Engl. transl. *Inorg. Mater. 23* (1988) 743.]
44. Tolochko, S. P., Kononyuk, I. F., Lyutsko, V. A. and Zonov, Yu. G. *Izv. Akad. Nauk SSSR, Neorg. Mater. 23* (1987) 1520. [Engl. transl. *Inorg. Mater. 23* (1988) 1342.]
45. Hewat, A. W. The Rietveld Computer Program for the Profile Refinement of Neutron Diffraction Powder Patterns Modified for Anisotropic Thermal Vibrations, UKAERE Harwell Report RRL 73/897 1973.
46. Thomas, M. W. and Bendoll, P. J. *Acta Crystallogr., Sect. A 34* (1978) 351.
47. Rietveld, H. M. *J. Appl. Crystallogr. 2* (1969) 65.
48. Köster, L. and Rauch, H. *IAEA Contract 2517/RB*, IAEA, Vienna 1981.
49. Watson, R. E. and Freeman, A. J. *Acta Crystallogr. 14* (1961) 27.
50. Bugge, R. Thesis, University of Oslo, Oslo 1996.
51. Brese, N. E. and O'Keeffe, M. *Acta Crystallogr., Sect. B 47* (1991) 192.
52. Altermatt, D. and Brown, I. D. *Acta Crystallogr., Sect. B 41* (1985) 240.
53. Shannon, R. D. *Acta Crystallogr., Sect. A 32* (1976) 751.
54. Andresen, A. F., Fjellvåg, H., Steinsvoll, O., Kjekshus, A., Stølen, S. and Bärner, K. *J. Magn. Magn. Mat. 62* (1986) 241.
55. Hauback, B. C., Fjellvåg, H. and Sakai, N. *J. Solid State Chem. 124* (1996) 43.
56. Yamaguchi, S., Okimoto, Y. and Tokura, Y. *Phys. Rev. B 55* (1997) R8666.
57. Taguchi, Y., Ichikawa, K., Katsumi, T., Jouda, K., Ohta, Y., Soda, K., Kawamata, S., Okuda, K. and Aita, O. *J. Phys. Condens. Matter 9* (1997) 6761.
58. Itoh, M., Mori, M., Sugahara, M., Yamauchi, T. and Ueda, Y. *Physica B 230–232* (1997) 756.
59. Takahashi, M. and Igarashi, J. *Phys. Rev. B 55* (1997) 13557.
60. Yamaguchi, S., Okimoto, Y. and Tokura, Y. *Phys. Rev. B 54* (1996) R11022.
61. Wu, Z. Y., Benfatto, M., Pedio, M., Cimino, R., Mobilio, S., Barman, S. R., Maiti, K. and Sarma, D. D. *Phys. Rev. B 56* (1997) 2228.
62. Fjellvåg, H., Gulbrandsen, E., Aasland, S., Olsen, A. and Hauback, B. C. *J. Solid State Chem. 124* (1996) 190.
63. Radaelli, P. G., Cox, D. E., Marezio, M. and Cheong, S. W. *Phys. Rev. B 55* (1997) 3015.
64. Taguchi, H. *J. Solid State Chem. 122* (1996) 297.

Received September 29, 1997.